High-precision reflectometer for submillimeter wavelengths

A. J. Gatesman, R. H. Giles, and J. Waldman

Submillimeter Technology Laboratory, University of Massachusetts Lowell, Lowell, Massachusetts 01854

Received April 11, 1994; revised manuscript received September 12, 1994

A high-precision reflectometer has been designed and implemented to measure directly the specular reflectance (R) of materials in the submillimeter (SM) region of the spectrum (300 GHz $< \nu <$ 3000 GHz). Previous laser-based measurement systems were limited to an uncertainty in R of $\pm 1.0\%$ because of a number of issues such as lack of an absolute reflection standard, difficulties in the interchange of sample and standard in the laser beam, and instabilities in the laser system. We realized a SM reflection standard by ellipsometrically characterizing the complex index of refraction of high-purity, single-crystal silicon to a precision such that its SM reflectivity could be calculated to better than $\pm 0.03\%$. To deal with alignment issues, a precision sample holder was designed and built to accommodate both sample and silicon reflection standard on an air-bearing rotary stage. The entire measurement system operated under computer control and included ratioing of the reflected signal to a reference laser signal, measured simultaneously, to help to eliminate short-term laser instabilities. Many such measurements taken rapidly in succession helped to eliminate the effects of both source and detector drift. A liquid-helium-cooled bolometer was modified with a large area detecting element to help to compensate for the slight residual misalignment between sample and reflection standard as they were positioned into and out of the laser beam. These modifications enabled the final measurement precision for R to be reduced to less than 0.1%. The major contribution to this uncertainty was the difficulty in precisely exchanging the positions of sample and standard into and out of the laser beam and was not due to laser or detector noise or instabilities. In other words, further averaging would not help to reduce this uncertainty. This order-of-magnitude improvement makes possible, for the first time to our knowledge, high-precision reflectance measurements of common metals such as copper, gold, aluminum, and chromium whose predicted reflectivities exceed 99% in the SM region. Furthermore, precise measurement of the high-frequency losses in high-temperature superconducting materials is now also possible. Measurements reported here of metals at a laser wavelength of $\lambda = 513.01$ μm ($\nu \approx 584$ GHz) indicate a slight discrepancy between experimental and theoretically predicted values, with measured results falling 0.1–0.3% below predicted values.

1. INTRODUCTION

As requirements of systems operating at millimeter (MM) and submillimeter (SM) frequencies become more demanding, accurate materials characterization at these frequencies becomes critical. Highly conductive materials such as metals and superconductors find important technological applications in communications, radar, and astronomy. From a scientific point of view, precise data are required for elucidating the fundamental nature of these materials.

The high-frequency properties of metals are of great technical importance. Discrepancies have been found to exist between measured and theoretical values of absorption [defined by Eq. (1) below] from the infrared into the microwave spectral regions. Since demanding communication, radar, and now astrophysical systems operate at these wavelengths, these discrepancies have become a problem. Differences were first observed at microwave (1–20-GHz) frequencies and later at MM (20–300-GHz) frequencies. They are relatively low at 10 GHz but can become appreciable in the MM-wave region above 30 GHz. Increases in absorption of 50–100% have been observed at 35 and 70 GHz.[1] For a dielectric material that exhibits loss (e.g., a metal), conservation of energy requires that the sum of reflected (R), transmitted (T), and absorbed (A) electromagnetic energy equal unity, i.e., $R + T + A = 1$. Unless the specimen is sufficiently thin there will be no transmission, and the absorption can be determined by measurement of the reflected intensity:

$$A = 1 - R\,. \tag{1}$$

Many times the quantity of interest is the real part of the complex surface impedance, or the surface resistance R_s. This quantity is proportional to A, and, for good conductors at low frequencies,

$$R_s = (Z/4)(1 - R)\,, \tag{2}$$

where Z is the impedance of the medium in which the measurement is made and is 376.99 Ω (mks units) for free space. A measurement of the reflectance can therefore be used to determine the surface resistance. The difficulty is that R_s of a good conductor is typically very small in the submillimeter (SM) region (<1 Ω^2/square) where the reflectance is near unity. From Eq. (2) we see that for a material with a reflectance of ≈99% an uncertainty in the reflectance of 1% leads to a ≈100% uncertainty in R_s. Therefore the reflectance of a highly conductive material should be measured to at least 0.1% to be useful. This fact is illustrated in Fig. 1, where we plot the theoretical reflectivity for several common metals, using the Hagen–Rubens (HR) relation[2] [Eq. (3) below]. Table 1 lists the resistivities and conductivities of these metals.

$$R_{\mathrm{HR}} = 1 - \sqrt{\frac{2\omega}{\pi\sigma_{\mathrm{dc}}}}\,. \tag{3}$$

0740-3224/95/020212-08$06.00

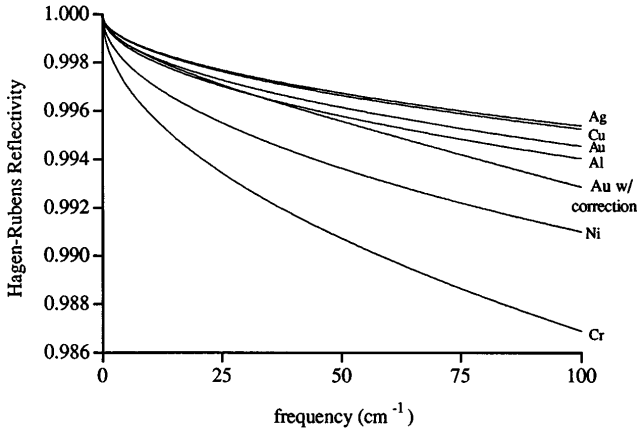

Fig. 1. HR reflectivity of metals listed in Table 1. The high-frequency correction described in Section 4 is shown for gold.

Table 1. Resistivities and Conductivities of Various Metals

Metal	Resistivity ($\mu\Omega$ cm)	T (K)	Conductivity ($\times 10^{17}$ s^{-1})	Drude Relaxation Time ($\times 10^{-14}$ s)
Silver	1.587	293	5.671	4.0
Copper	1.678	293	5.364	2.7
Gold	2.214	283	4.065	3.0
Aluminum	2.650	293	3.396	0.8
Nickel	6.03	293	1.49	0.65
Chromium	12.9	273	0.70	0.17

The HR relation predicts a reflectivity dependent only on the angular frequency ω of the incident radiation and the dc conductivity of the metal, σ_{dc}. It does not take any frequency dependence of the conductivity into account. In reality, as the frequency is increased (from microwave to SM frequencies), the ac conductivity of a metal becomes complex, and the HR relation begins to break down. A more exact theory, outlined in Section 4 below, accounts for the conductivity's complex behavior and predicts a reflectivity lower than predicted by Eq. (3). In other words, the HR relation underestimates the high-frequency loss in a metal.

This research was motivated by the fact that the SM frequency regime lacks a precise, straightforward means of measuring the reflectance of materials. The reflectometer described here was based on a CO_2 optically pumped SM laser system. Practically, the SM region of the spectrum (100 μm $< \lambda <$ 1000 μm) is the longest wavelength region for which straightforward, free-space optical techniques can be used. Components such as front surface mirrors, lenses, beam splitters, polarizers, and wave plates that are routinely employed at shorter wavelengths can be used equally as well in the SM region. At wavelengths longer than $\approx$1–2 mm, diffraction prevents one from performing extremely precise optical measurements in a simple, free-space manner. On the other hand, SM frequencies are low enough to permit us to gain insight into the low-frequency (i.e., microwave, MM-wave) behavior of materials. Previous laser-based measurement systems were limited to an uncertainty in R of approximately 1.0% for a number of reasons, such as difficulty in the interchange of sample and standard in the laser beam, instabilities in the laser system, and lack of an absolute reflection standard. This research addresses all these problems.

The measurement of the reflected intensity of a specimen at SM wavelengths is typically a relative measurement. The accuracy achieved ultimately rests on the assumptions concerning the reflective properties of the reference standard and how well it can be exchanged with a test sample in the measurement system. Long-wavelength reflectance measurements are commonly made by comparison with a metal typically in the form of a thin film that is assumed to have a reflectivity of unity. Unless the film is of high quality and sufficiently thick to avoid skin depth problems, its reflectance may depart significantly from unity. There is also the problem that the high-frequency properties of metals may not be well defined. At some frequency the skin effect will become anomalous and the metal's reflectance will depart from predictions of the simple theory (such as the Drude theory). Therefore, for precise measurements, reference to a metal surface is invalid. The technique used here relies on the fact that the reflectivity of a solid specimen can be calculated more accurately than measured if its optical constants are known with sufficient precision. We realized a SM reflection standard by ellipsometrically characterizing the complex index of refraction of high-purity, single-crystal silicon to a precision such that the SM reflectivity of a silicon étalon could be calculated to better than $\pm$0.03%. This idea was apparently first used by Birch.[3] To deal with alignment issues, a precision sample holder was designed and built to accommodate both sample and silicon standard on a computer-controlled rotary stage. The precision sample holder enabled specimens to be mounted with an angle-of-incidence repeatability of $\leq$0.03°. Several ball- and cross-roller-bearing rotary stages were tested and found to exhibit appreciable wobble. To deal with this issue, an air-bearing rotary stage was implemented to position both test sample and silicon étalon reflection standards into and out of the laser beam. A liquid-helium-cooled bolometer was modified with a large-area detecting element to help to compensate for the slight residual misalignment between sample and standard as they were positioned into and out of the laser beam.

Several real-time computer averaging techniques were necessary to help to compensate for both short- and long-term instabilities inherent in the SM laser. Raw laser output contained nonrandom fluctuations in power of $\approx$1% and long-term drift (of the order of several minutes) of 10–15% as a result of vibrations, changes in room temperature and humidity, etc. A reference bolometer continuously monitored the laser's output power. An electronic ratiometer simultaneously ratioed outputs of signal and reference detectors and therefore helped to compensate for short-term drifts. Long-term drifts were dealt with by repetition of many measurements rapidly in succession over an $\approx$6-min period and then averaging of the complete data set for the final result.

Several metal films were examined with the precision reflectometer. High-conductivity metals such as gold, aluminum, and copper have theoretical (HR) reflectivities that range from $\approx$99.5% to 99.9% in the SM, as shown in Fig. 1. The final measurement system was able to mea-

sure the difference in reflectance among these metals. This significant achievement permits, for the first time to our knowledge, the study of highly reflecting materials in the SM region of the spectrum. High-precision, room-temperature reflectance data at 584 GHz are presented for a variety of metals and are compared with theoretical predictions.

2. REFLECTION STANDARD

The reflectivity of any standard considered had to be calculable to high precision given quantities such as the material's complex index of refraction ($n + ik$, where n is the refractive index, i is $\sqrt{-1}$, and k is the extinction coefficient) and angle of incidence and the laser wavelength. A well-studied material in the SM with this potential is single-crystal, high-purity silicon. Silicon was chosen in preference to germanium because of phonon bands that have been observed in germanium at wavelengths as long as 100 μm. Also, the fact that the band gap in germanium is nearly half that of silicon's leads to a far greater number of carriers thermally excited across the band gap into the conduction band at room temperature. These features cause structure in germanium's SM optical properties that are best avoided in this application.

Single-crystal silicon has several attractive features, such as very low dispersion, availability in ultrahigh purities, and the ability to be polished optically to a precise thickness. Birch[3] appears to have been the first to apply silicon as a precision reflection standard in the SM region. His characterization consisted of spectroscopic measurements from 5 to 120 cm^{-1} ($\lambda \approx 2$ mm-83 μm) on a 1000-Ω cm silicon wafer, using the technique of dispersive Fourier-transform spectroscopy. His results for the complex index of refraction show n decreasing and α, the power absorption coefficient ($\alpha = 4\pi k/\lambda$), increasing with wavelength. An increase in α with SM wavelength in semiconductors is usually indicative of absorption that is due to free carriers. As mentioned above, it is desirable to work with material that exhibits as little dispersion as possible. One way to limit the number of free carriers and hence the dispersion in α is to use a high-resistivity (high-purity) material.

The SM optical properties of high-resistivity silicon have been studied in Grischkowsky *et al.*,[4] who used time-domain spectroscopy to measure the absorption and dispersion in several dielectrics and semiconductors. Their data on >10,000-Ω cm silicon displays low dispersion and a power absorption coefficient that decreases with wavelength at $\lambda = 200-1000$ μm. A small decrease in α with wavelength is theoretically expected because of the residual effects of the wing of the infrared lattice absorption bands and indicates no measurable contribution from free-carrier absorption. Therefore, in this work, high-resistivity (40,000–60,000-Ω cm) 2.54-cm-diameter, p-type silicon was employed as the material for the precision reflection standard.

The basic design of the reflection standard was in the form of an étalon. It is advantageous to work with an étalon with a relatively low optical thickness (the product of the physical thickness t and the real part of the complex index of refraction n), because uncertainty in the thickness will then have a smaller effect on calculated values of R. The optical thickness is controlled by adjustment of t. It is also obvious that the thickness should be adjusted such that a reflectivity maximum occurs at the laser wavelength of interest. Assuming that the étalon's thickness was designed in this way, one needs to know precisely how the uncertainties in the measured quantities n, k, and t correlate to uncertainty in the calculated reflectivity. One can show that the maximum allowable uncertainties in n, k, and t (for an étalon $\approx$400 μm thick) are ± 0.002, ± 0.0001, and ± 1.0 μm, respectively, if one wishes to calculate the reflectivity to better than 0.1%.[5] Even near normal incidence, the polarization and the angle of incidence i affect the reflectivity. The p-polarized reflectivity begins to decrease with incident angle (this is the polarization in which Brewster's angle is observed) and the s-polarized reflectivity begins to increase, eventually reaching unity along with the p polarization at $i = 90°$. The angle of incidence should be known to within $\approx 0.5°$ (for $i < 5°$) if one wishes to calculate the reflectivity to better than 0.1%. The equations used to determine the above tolerances are the familiar Fresnel equations as given in Ref. 6.

Using ellipsometric techniques,[7] we measured the complex index of refraction of the silicon at $\lambda = 513.01$ μm; it is given in Table 2. The uncertainty in n and k when this technique is used is within the maximum allowable uncertainties mentioned above. Polishing of the 2.54-cm-diameter silicon into a 413.0-μm étalon with an uncertainty in thickness of ± 0.25 μm was performed by Kappler Crystal Optics, Holliston, Massachusetts. One can again use the Fresnel equations to predict the reflectivity of a silicon étalon at this wavelength. The predicted Fresnel reflectivity for s-polarized radiation at an angle of incidence of 1.9° and at $\lambda = 513.01$ μm was 0.7093. When precise reflectance measurements are made at nonnormal angles of incidence, it is necessary to consider the spherical-Gaussian nature of the SM laser beam to account for the incomplete overlap of multiple internal reflections that occurs within the étalon.[8] It turns out, however, that at an incident angle of 1.9° the difference in reflectivity when one accounts for the spherical-Gaussian nature and when one does not account for this effect is <0.01% (Ref. 5) and therefore can safely be ignored here.

3. EXPERIMENT

A. Measurement System

We made reflectance measurements of several metals, using the high-precision reflectometer described here. The metals that were studied included copper, silver, gold,

Table 2. Ellipsometrically Determined SM Complex Index of Refraction of Silicon ($\rho_{dc} = 40-60$ kΩ cm)

Wavelength (μm)	Frequency (cm^{-1})	Refractive Index (n)	Extinction Coefficient (k)		Absorption Coefficient (cm^{-1})	
513.0157	19.4926	3.4164 ± 0.0002	0.00004	+0.00008 −0.00004	0.01	+0.02 −0.01

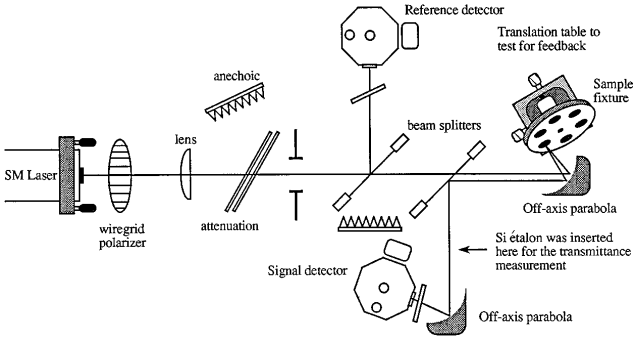

Fig. 2. General optical configuration of the high-precision reflectometer showing signal and reference detectors (liquid-helium bolometers) and the six-position sample holder mounted on an air-bearing rotary stage.

aluminum, nickel, and chromium. These metals were positioned in a custom-built sample holder, which was mounted on an air-bearing rotary stage. A schematic of the optical system is shown in Fig. 2. The sample holder–air-bearing assembly was designed to give a smooth, wobble-free, repeatable exchange of sample and standard into and out of the laser beam. The air-bearing rotary system was chosen over more conventional ball- and cross-roller-bearing rotary stages because of its superior performance. Air bearings have minimal wobble and radial runout, which are best avoided in this application. The sample holder accommodated the silicon étalon reflection standard and as many as five test pieces. Samples and standard were mounted in the holder with small springs to ensure that they were pressed flat against the ground flat surface of the holder's top mounting plate. This procedure ensured that all reflecting surfaces were located in the same plane.

The metal films were obtained from a variety of sources. Thin Film Lab, West Hurley, New York, provided films of copper, silver, gold, nickel, and chromium. All these except gold had an ≈25-nm protective layer of SiO_2 to prevent oxidation and scratching. These films were deposited with an *e*-beam deposition system to thicknesses ≥400 nm on 2.54-cm-diameter BK-7 glass substrates with 80/50 surface quality. Deposition parameters such as base pressure, temperature, and deposition rate were set to optimize the film's performance at optical frequencies. The aluminum films were deposited by PFG Precision Optics, Ocean Springs, Mississippi, to a thickness of ≥300 nm with an ≈25-nm SiO protective overcoating. Typical skin depths of common metals at 584 GHz are ≈100 nm. The remaining films were enhanced aluminum, protected aluminum, and gold mirrors from Edmund Scientific. Edmund's protected aluminum mirrors are overcoated with ≈55 nm of SiO. The enhanced aluminum is overcoated with an ultraviolet-transmitting dielectric (MgF_2) to extend its use into the ultraviolet. The absorption of these protective coatings was calculated to have a negligible effect ($<10^{-4}$) in the SM region.

The signal and reference detectors were liquid-helium-cooled bolometers. We modified the signal bolometer by removing its internal parabolic collection cone and replacing the 2 mm × 2 mm detecting element with a large-area element (12-mm diameter) to help to compensate for any residual misalignment between sample and standard. For the given optical configuration described below, an assumed 10% spatial nonuniformity in the detecting element's responsivity leads to a negligible effect on the overall measurement uncertainty (i.e., it contributes less than ≈0.02% uncertainty). Two off-axis parabolic reflectors were used to focus the radiation on both the sample and the detecting element. The sample under test was placed at the focus of the off-axis parabolic mirror. The waist size ($1/e^2$ intensity) of the SM laser beam at the sample surface was calculated to be less than 2λ. Two samples not in identical alignment had reflected rays that diverged until they reflected from the off-axis parabola, where they then reflected as parallel rays. The two rays would then remain parallel along their path (≈35″) toward the detector's off-axis parabola. The detecting element was placed near the focus of its off-axis parabola. This arrangement was necessary to yield high-precision results that would not have been possible if lenses were employed.

A problem commonly encountered in systems with coherent sources is the standing waves (feedback) that exist between the various components of the optical system (e.g., the laser resonator and reflecting sample). Coherent feedback effects are easily observed when one is working at normal incidence by translating the reflecting sample into and out of the direction of the oncoming radiation (see Fig. 2) and observing a (≤10%) modulation at the signal detector. To help to minimize this problem, reflectance measurements were made slightly off normal incidence (≈1.9°). To reduce coherent feedback effects further, attenuation (acrylic plastic) was inserted at the laser's output and in front of the signal and reference detectors. Though this attenuation reduced the demodulated signals to ≈10 mV, compared with 1 V without attenuation, it eliminated the feedback problem. Feedback diminishes with attentuation faster than signal does because signal loss is a single-pass loss, whereas feedback suffers from a double-pass loss. We verified that feedback had been suppressed by translating the sample fixture as described above and observing no signal modulation. The attenuated laser signal remained far above the detector noise, so that the latter had no effect on the measurements.

The laser system used was a CO_2 optically pumped SM laser. The 85-W CO_2 laser (mechanically chopped at 100 Hz) pumped the $\lambda = 513.01$-μm transition in a 2.7-m, 11.43-cm-diameter formic acid (HCOOH) gas-filled (100-mTorr) cavity. Radiation was coupled out of the cavity through an 8-mm-hole output coupler. This produced a high-quality, stable TEM_{00} Gaussian mode. Sidelobes on the main transmitted SM laser beam were typically between 18 and 22 dB down from the central maximum, as confirmed by spatial mode scans of the beam's cross section. The overall stability of the CO_2–SM laser system was an important factor in the measurement procedure. The CO_2 laser was actively stabilized by a Fabry–Perot frequency-locking system.[9] This device monitored the frequency of the CO_2 laser and actively made minor adjustments to the laser's cavity length to keep the CO_2 frequency constant. There was no active stabilization on the SM laser. Its output power would slowly drift owing to changes in the laser cavity length caused by thermal fluctuations in the room (e.g.,

cycling of the air conditioner). This cyclic behavior resulted in a 10–15% variation in laser output power every ≈20 min. Most other sources of noise were short term in nature and had to be dealt with accordingly. Short-term fluctuations can be a result of a variety of sources such as mechanical vibrations, power supply (electrical) noise, CO_2–SM feedback, and changes in environmental conditions (such as humidity) along the various beam paths. Several techniques were implemented to minimize these effects and maximize overall system performance. As is shown in Fig. 2, a reference detector monitored the SM laser's output power. Two lock-in amplifiers demodulated both signal and reference detector outputs. The output of the signal's lock-in was continually ratioed to the reference's lock-in output by an electronic ratiometer. The comparison is essentially instantaneous if one assumes that the two lock-ins have identical response characteristics. The technique of ratioing was critical in achieving high-precision results. Ratiometer output was input to one of the analog-to-digital converter channels of the signal lock-in to be read by the computer. Several different lock-in time constants were tested, and 100 ms was found to be optimal. The entire measurement system was automated under computer control.

Even though the étalon's reflectance could not be measured with high precision, its transmittance (T) could be. This is because the standard for a transmittance measurement is air with an assumed complex index of refraction of $1.0 + i0.0$. The theoretically calculated transmissivity of the étalon at $\lambda = 513.01$ μm and $i = 1.9°$ is 0.29044. Though it would have been desirable to measure T at this angle of incidence, feedback prevented this. A transmittance measurement was therefore performed at an angle of incidence of $i = 8.5°$. The theoretically predicted value for the transmissivity at 8.5° is 0.28581. The optical configuration for this measurement was the same as that for the reflectometer setup, except that the silicon étalon was inserted as indicated in Fig. 2. The experimentally measured value of 0.2861 is very close to the transmissivity predicted above. This measurement provided experimental verification that the silicon étalon had indeed been designed properly as a reflection standard. After samples and standard were inserted into the fixture, we checked their relative alignment by backreflecting a He–Ne laser onto a far wall. After several measurements of two nominally identical gold mirrors it was determined that the relative angular alignment of samples should be ≤0.03° to yield better than ±0.1% uncertainty in the reflectance. Therefore, before each measurement sequence, this relative alignment was checked and verified. Also, just before the measurements, two nominally identical gold mirrors were inserted, and measurements were made to verify that the system measured a ratio of 1.000 ± 0.001 or better.

B. Measurement Procedure and Data

A measurement sequence consisted of the following steps:

1. The rotary stage was positioned so that the laser reflected from the metal film under test.
2. Several ratiometer outputs were acquired every ≈10 ms in an ≈100-ms interval and averaged.
3. The rotary stage rotated to the silicon étalon reflection standard.
4. Several ratiometer outputs were again acquired every 10 ms in an ≈100-ms interval and averaged.
5. The rotary stage was positioned back to the metal film.

Because residual short-term noise still existed on the ratiometer output, it was necessary to acquire several ratioed outputs within a short (≈100-ms) time interval and then average the results. The above procedure was performed 50 times over an ≈6-min period (i.e., the reflectance was measured 50 times), and the mean and the standard deviation of the data set were calculated.

Data for copper, silver, gold, aluminum, nickel, and chromium are summarized in Table 3. Values of the reflectivity calculated with the HR relation [Eq. (3)] and its high-frequency correction (given in the Section 4) are also presented. Data for commercially available front surface mirrors are given in Table 4. The overall uncertainty in the measurements was ±0.1%. This error is due almost exclusively to positioning error (i.e., the inability precisely to interchange metal film and silicon étalon into and out of the laser beam).

Table 3. Results of Reflectivity Measurements at $\lambda = 513.01$ μm

Metal	Reflectivity at 513.01 μm	Uncertainty	HR Eq. (3)	HR with Correction Eq. (4)	Conductivity ($\times 10^{17}$ s^{-1})	Relaxation Time ($\times 10^{-14}$ s)
Copper	0.997	0.001	0.9979	0.9978	5.36	2.70
Silver	0.996	0.001	0.9980	0.9978	5.67	4.00
Gold	0.994	0.001	0.9976	0.9975	4.07	3.00
Aluminum	0.995	0.001	0.9974	0.9973	3.40	0.80
Nickel	0.994	0.001	0.9960	0.9960	1.49	0.32
Chromium	0.993	0.001	0.9942	0.9942	0.70	0.33

Table 4. Reflectivity of Commercially Available Front Surface Mirrors

Metal	Reflectivity at 513.01 μm	Uncertainty	HR Eq. (3)	HR with Correction Eq. (4)	Conductivity ($\times 10^{17}$ s^{-1})	Relaxation Time ($\times 10^{-14}$ s)
Enhanced aluminum	0.992	0.001	0.9974	0.9973	3.40	0.80
Protected aluminum	0.985	0.001	0.9974	0.9973	3.40	0.80
Edmund gold	0.995	0.001	0.9976	0.9975	4.07	3.00

4. DISCUSSION

The use of a high-purity silicon étalon as a precision standard for reflectance measurements in the SM region has been demonstrated. Originally several reflection standards had been designed at a variety of SM wavelengths (which was possible because the silicon had been ellipsometrically characterized at a variety of SM wavelengths). The difficulty in designing an étalon at a shorter laser wavelength (e.g., $\lambda = 117.7\ \mu$m) is that the silicon's absorption begins to contribute significantly to its reflectivity and therefore to the overall uncertainty in the étalon's reflectivity. The absorption at $\lambda = 117.7\ \mu$m is roughly three times that at $\lambda = 513.01\ \mu$m. One way around this problem is to design a thinner étalon. A thinner étalon will also help to reduce the uncertainty in reflectivity attributable to uncertainty in refractive index n and thickness. However, attempts to polish the 2.54-cm-diameter silicon wafers to thickness less than $\approx 400\ \mu$m were unsuccessful.

A. Discrepancies

Reflectance data in Table 3 indicate a slight discrepancy between experimental and theoretical values. Measured results fall 0.1–0.3% below predicted values for all metals studied. For metals that are expected to be most free-electronlike (copper, silver, gold, aluminum), the average difference between experimental and theoretical (HR) values is ≈0.2%. As mentioned in Section 1, the HR relation does not take the complex nature of a metal's conductivity into account. It assumes that $\sigma(\omega) = \sigma_{\mathrm{dc}}$, which essentially says that $\omega\tau \ll 1$, where τ is the mean free collision time of the conduction electrons in the metal. In the general case, without any condition imposed on the value of $\omega\tau$, the reflectivity of a metal is given by[5]

$$R = 1 - \sqrt{\frac{2\omega}{\pi\sigma_{\mathrm{dc}}}}\left[(1 + \omega^2\tau^2)^{1/2} + \omega\tau\right]^{1/2}. \tag{4}$$

The extra term in brackets in Eq. (4) is ≥1 for $\omega\tau \geq 0$ and therefore predicts a greater loss than predicted by the HR relation alone. However, at 584 GHz, for typical values of τ, the difference in reflectivity predicted by Eqs. (3) and (4) is ≤0.02% (as seen in Tables 3 and 4 and Fig. 1) and therefore cannot explain the discrepancies seen here. This difference does become larger at higher frequencies, as expected. At 2.5 THz ($\lambda \approx 120\ \mu$m), differences are as large as 0.15%.

Discrepancies between experimentally measured values and theoretical predictions of high-frequency (i.e., microwave–SM) absorption in metals have been a long-standing problem. Batt *et al.*[10] have carefully investigated the surface resistance of gold at 890 GHz. Their technique involved evaporating a thin film of gold onto the front surface of a pyroelectric detector element. The modified detector was used in the normal way to produce a pyroelectric voltage proportional to the absorbed power of incident SM radiation. The ratio of actual-to-theoretical surface resistance is ≈2.2 when Eqs. (2) and (3) and the bulk conductivity of gold are used. Similar studies of copper and silver between 10 and 200 GHz also display measured-to-theoretical losses approaching 2.5.[11,12] Tischer[13] has investigated the attenuation of commercially available waveguides and has measured a loss ratio of 1.135 ± 0.02 for copper surfaces that were carefully prepared by electropolishing and annealing in hydrogen.

Many times, some portion of a discrepancy can be attributed to the preparation of the surface under test. Thorpe[14] has shown that the electrical properties of copper are a sensitive function of surface preparation. To maximize the conductivity he found it necessary to acid etch and then anneal the copper surfaces at 780 °C in a hydrogen environment. By this method an improvement in loss ratio from 1.32 to 1.01 at 38 GHz was observed. Hinderks and Maione[15] report near-theoretically predicted values of R_s for electrodeposited copper at 43 GHz. Their research shows that significant improvement in copper conductivity can be obtained through an annealing step and have reported a measured-to-theoretical loss ratio of 1.04.

At frequencies above the MM-wave region bulk samples are no longer necessary, and specimens that are sufficiently thick can be prepared by vacuum deposition. Thin metal films are generally preferred over prepared bulk metal surfaces for the study of optical properties; however, they are not without limitations. It has been shown that the SM surface resistance can depend on deposition parameters such as temperature. For aluminum films deposited into diamond substrates, Schiever *et al.*[16] have shown that a substrate temperature of 100–120 °C yields a film with a resistance at 105.55 GHz approaching theoretical values. On the other hand, for films deposited at room temperature, loss ratios as high as ≈2.5 are found. This implies that a material that normally reflects 99.7% in the SM region will reflect only 99.5%, or a reduction of approximately 0.2%. Because of this fact, any future research on metal films with this instrument should concentrate on studying the relationship between a film's preparation and its reflectance.

B. Application of SM Reflectometry to the Study of High-Temperature Superconductors

SM reflectometry has been shown to be a practicable technique to measure precisely the reflectance of metals. There is also current interest in the SM optical properties of superconductors.[17] Since the advent of superconductors with transition temperatures (T_c) above 77 K, these materials have generated much interest among microwave and MM-wave engineers. A current frequency limit in microwave circuits is ohmic loss. In addition to reducing ohmic loss, a circuit made from superconducting materials will have lower dispersion. Superconductors, unfortunately, have zero resistance only to dc currents. The surface resistance varies as ω^2, predicted by the London equations, which describe electron transport in the superconducting state, in contrast to normal metals whose surface resistance varies as $\omega^{1/2}$, predicted by the classical theory. Therefore, beyond some critical frequency (f_c), a normal metal will have a lower surface resistance than will a superconductor. At present bulk superconducting materials have critical frequencies of ≈10 GHz when compared with copper at 77 K.

However, recent measurements appear to show that thin-film high-temperature superconductors (HTS's) have f_c values beyond 100 GHz. Klein *et al.*[18] have measured

the MM-wave surface resistance of $YBa_2Cu_3O_{7-x}$ thin-film superconductors at 86.7 GHz and 77 K. Results indicate that R_s is nearly 1 order of magnitude less than the R_s of copper at 77 K and nearly equal to that of niobium at 7.7 K. As the HTS's continue to improve it will become increasingly difficult to determine their surface resistance at these frequencies. Most published measurements at MM-wave frequencies use cylindrical resonators and determine R_s from the cavity Q. In the measurement of a superconducting material the normal metal sides of the resonator should have as little resistance as possible, and the HTS should make up as much of the resonator's walls as possible. Accuracy in determining R_s will typically be poor if the material under study has a lower R_s than that of the material that composes the rest of the resonator. This is the case for a high-quality thin-film superconductor measured by use of a resonator made of copper. Ideally, the resonator should be constructed from superconducting material itself, which is not practical. One way to approach this problem is to measure R_s at higher frequencies, where losses are much greater, and scale the results to the MM-wave region. According to the BCS theory, the surface resistance of a superconductor below the gap frequency increases as the square of the frequency. This has been experimentally verified for HTS.[19,20] One can use a SM reflectometer to determine R_s at SM frequencies, using Eq. (2), and then scale R_s to microwave frequencies, using ω^2 scaling. The uncertainty in the SM surface resistance in ohms/square is approximately equal to the uncertainty in the reflectivity, ΔR, in percent. Therefore an uncertainty $\Delta R \approx 0.1\%$ leads to a ΔR_s of $\approx 0.1\ \Omega$/square. The sensitivity at 10 GHz implied by ω^2 scaling of R_s (measured at 1.5 THz) is therefore $\approx 4\ \mu\Omega$/square. The SM technique is therefore more sensitive than common microwave measurements. Uncertainties in parallel-plate resonator techniques are typically $\pm 20\ \mu\Omega$/square at 77 K and $\pm 60\ \mu\Omega$/square at 95 K.[21] End-wall replacement techniques suffer even greater uncertainties (a few milliohms) because of the metallic walls of the cavity.

Also of current interest is the ability to spatially scan the surface of a superconducting material. As thin-film superconducting samples increase in size, the ability to measure the spatial distribution of R_s becomes of interest. The waist of the SM laser used in experiments described above was ≈ 0.7 mm at $\lambda = 513.01\ \mu$m. At shorter wavelengths smaller waist sizes would be possible. These near-diffraction-limited spot sizes could make high-spatial-resolution measurements of the surface resistance possible.

5. CONCLUSION

A high-precision reflectometer has been designed and built to operate in the SM region of the spectrum. Problems such as sample positioning, lack of an absolute reflection standard, and instabilities in the SM laser system that typically limit measurement precision have been investigated. Critical in this effort was the optical characterization of a high-purity silicon wafer such that an étalon fabricated from this material had a calculable SM reflectivity with an uncertainty of less than $\pm 0.03\%$. This was achieved by use of an ellipsometer specifically designed for materials characterization at SM wavelengths. Sample positioning was achieved through construction of a specially designed sample fixture, which was mounted on an air-bearing rotary stage. These efforts reduced the overall uncertainty in reflectance from $\pm 1\%$ achieved in previous systems to less than $\pm 0.1\%$. This order-of-magnitude improvement makes possible, for the first time to our knowledge, high-precision reflectance measurements of materials in the SM region. The differences in reflectance among common metals, which are of the order of several tenths of 1%, can now be discerned. We measured the absolute reflectance of several thin metal films at $\lambda = 513.01\ \mu$m, using the silicon étalon standard. The data indicate a slight discrepancy between experimental and theoretical values, with measured results falling 0.1–0.3% below values predicted by the simple theory. This discrepancy has been observed as well in the SM and MM-wave frequency regions by other researchers. High-precision reflectometry can also be used as a sensitive technique to measure the surface resistance of high-temperature superconducting materials as well as to study the relationship between the preparation of a metal film and the reflectance of the film.

ACKNOWLEDGMENTS

This paper is based on material submitted by A. J. Gatesman for the degree of doctor of philosophy at the University of Massachusetts Lowell.

This research was supported in part by the U.S. Army National Ground Intelligence Center and Xsirius Superconductivity, Inc. The authors thank D. Cohn and P. Woskov for pointing out the importance of high-precision reflectometry to the study of superconductors.

REFERENCES

1. F. J. Tischer, "Excess surface resistance due to surface roughness at 35 GHz," IEEE Trans. Microwave Theory Tech. **22,** 566–569 (1974).
2. B. Donovan, *Elementary Theory of Metals* (Pergamon, London, 1967), Chap. 9.
3. J. R. Birch, "The absolute determination of complex reflectivity," Infrared Phys. **18,** 613–620 (1978).
4. D. Grischkowsky, S. Keiding, M. van Exter, and Ch. Fattinger, "Far-infrared time-domain spectroscopy with terahertz beams of dielectrics and semiconductors," J. Opt. Soc. Am. B **7,** 2006–2015 (1990).
5. A. J. Gatesman, "A high precision reflectometer for the study of optical properties of materials in the submillimeter," Ph.D. dissertation (University of Massachusetts Lowell, Lowell, Mass., 1993).
6. R. M. A. Azzam and N. M. Bashara, *Ellipsometry and Polarized Light* (Elsevier/North Holland, Amsterdam, 1977), Chap. 4.
7. R. H. Giles and M. J. Coulombe, "Design of a submillimeter ellipsometer for the measurement of the complex indices of refraction of materials," in *Proceedings of the 10th International Conference on Infrared and Millimeter Waves* (Institute of Electrical and Electronics Engineers, New York, 1985), pp. 319–320.
8. J. C. Cotteverte, F. Bretenaker, and A. Le Floch, "Jones matrices of a tilted plate for Gaussian beams," Appl. Opt. **30,** 305–311 (1991).
9. J. L. Pelletier, "Frequency locking system for a CO_2 laser," M.S. thesis (University of Massachusetts Lowell, Lowell, Mass., 1990).

10. R. J. Batt, G. D. Jones, and D. J. Harris, "The measurement of the surface resistivity of gold at 890 GHz," IEEE Trans. Microwave Theory Tech. **MTT-25,** 488–491 (1977).
11. F. A. Benson, *Millimeter and Submillimeter Waves* (Iliffe, London, 1969), Chap. 14.
12. N. Marcuvitz, *Waveguide Handbook* (McGraw-Hill, New York, 1951).
13. F. J. Tischer, "Excess conduction losses at millimeter wavelength," IEEE Trans. Microwave Theory Tech. **MTT-24,** 853–858 (1976).
14. T. S. Thorpe, "Rf conductivity in copper at 8 mm wavelengths," Proc. Inst. Elec. Eng. Part 3 **101,**357–359 (1954).
15. L. W. Hinderks and A. Maione, "Copper conductivity at millimeter-wave frequencies," Bell Syst. Tech. J. **59,** 43–65 (1980).
16. K. S. Schiever, J. M. Baird, L. R. Barnett, and R. W. Grow, "Investigation of techniques for minimizing resistivity of thin metallic films at submillimeter wavelengths," Int. J. Infrared Millimeter Waves **13,** 1139–1143 (1992).
17. P. P. Woskov, D. R. Cohn, S. C. Han, R. H. Giles, and J. Waldman, "Precision submillimeter-wave reflectometry of metals and superconductors," presented at the 15th International Conference on Infrared and Millimeter Waves, Lake Buena Vista, Fla., December 10–14, 1990.
18. N. Klein, G. Muller, H. Piel, B. Roas, L. Shultz, U. Klein, and M. Peiniger, "Millimeter wave surface resistance of epitaxially grown $YBa_2Cu_3O_{7-x}$ thin films," Appl. Phys. Lett. **54,** 757–759 (1989).
19. D. Miller, P. L. Richards, S. Etemad, A. Inam, T. Venkatesan, B. Dutta, X. D. Wu, C. B. Eom, T. H. Geballe, N. Newman, and B. F. Cole, "Residual losses in epitaxial thin films of $YBa_2Cu_3O_7$ from microwave to submillimeter wave frequencies," Appl. Phys. Lett. **59,** 2326–2328 (1991).
20. J. S. Martens and J. B. Beyer, "Microwave surface resistance of $YBa_2Cu_3O_{6.9}$ superconducting films," Appl. Phys. Lett. **52,** 1822–1824 (1988).
21. W. L. Holstein, L. A. Parisi, C. Wilker, and R. B. Flippen, "$Tl_2Ba_2CaCu_2O_8$ films with very low microwave surface resistance up to 95 K," Appl. Phys. Lett. **60,** 2014–2016 (1992).